

Sweet Child O' Mine—where do we go now? In *C. elegans*, NAC prevents vacant ribosomes and ribosome-nascent chain complexes (RNCs) translating cytoplasmic or mitochondrial proteins from mistargeting to the ER membrane. Upon depletion of NAC activity, the proofreading activity of the Sec61 translocon suffices to prevent cytoplasmic proteins, but not many mitochondrial proteins, from import into the ER.

The *in vivo* work by Gamerdinger *et al.* establishes and further defines a central process in protein biogenesis for metazoan cells, and corroborates much of the earlier *in vitro* work done by Wiedmann. Systematic approaches such as proteome-wide interaction profiling of nascent chains are now needed to elucidate the dynamics and interplay of SRP, NAC, and other ribosome-associated factors at the ribosome. Finally, the Deuerling-Wiedmann model (see the figure) of antagonistic “sort and countersort” reflects a recurring principle of check and countercheck common to a number of biological mechanisms. Such systems provide a calibrated equilibrium between two opposing functions that enhances accuracy and efficiency in decision-making processes within living cells. ■

PROTEIN TARGETING

The principle of antagonism ensures protein targeting specificity at the endoplasmic reticulum

Martin Gamerdinger,¹ Marie Anne Hanebuth,¹ Tancred Frickey,² Elke Deuerling^{1*}

The sorting of proteins to the appropriate compartment is one of the most fundamental cellular processes. We found that in the model organism *Caenorhabditis elegans*, correct cotranslational endoplasmic reticulum (ER) transport required the suppressor activity of the nascent polypeptide-associated complex (NAC). NAC did not affect the accurate targeting of ribosomes to ER translocons mediated by the signal recognition particle (SRP) pathway but inhibited additional unspecific contacts between ribosomes and translocons by blocking their autonomous binding affinity. NAC depletion shortened the life span of *Caenorhabditis elegans*, caused global mistargeting of translating ribosomes to the ER, and provoked incorrect import of mitochondrial proteins into the ER lumen, resulting in a strong impairment of protein homeostasis in both compartments. Thus, the antagonistic targeting activity of NAC is important in vivo to preserve the robustness and specificity of cellular protein-sorting routes.

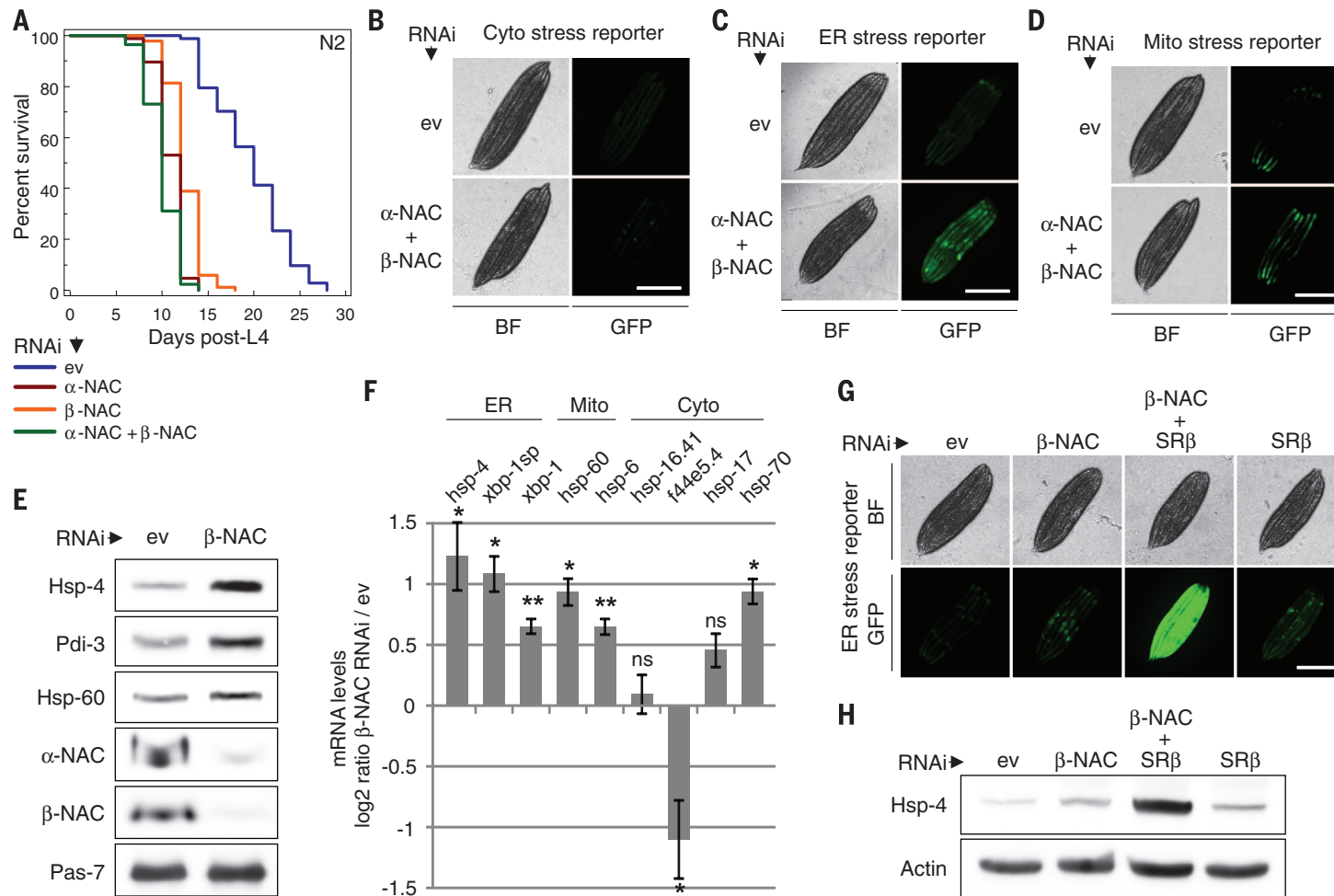


Fig. 1. NAC depletion shortens adult life span and induces stress in the ER and mitochondria.

(A) Life span survival curves of N2 worms grown at 20°C on empty vector control (ev, blue; median life span 20 days), α -NAC RNAi (red; median life span 12 days), β -NAC RNAi (orange; median life span 10 days), or α -NAC + β -NAC RNAi (green; median life span 10 days). (B) *hsp-16.2p::GFP* cytosolic stress reporter worms were grown on empty vector control (ev) or α -NAC + β -NAC RNAi. GFP fluorescence was assessed on day 3 of adulthood (fig. S1, A and B). BF, bright-field. Scale bar, 0.5 mm. (C) *hsp-4p::GFP* ER stress reporter worms were grown on empty vector control (ev) or α -NAC + β -NAC RNAi, and GFP fluorescence was assessed on day 3 of adulthood (fig. S1C). BF, bright-field. Scale bar, 0.5 mm. (D) *hsp-6p::GFP* mitochondrial stress reporter worms were grown on empty vector control (ev) or α -NAC + β -NAC RNAi, and GFP fluorescence was assessed on day 2 of adulthood (fig. S1D). BF, bright-field.

Scale bar, 0.5 mm. (E) N2 worms were grown on empty vector control (ev) or β -NAC RNAi. On day 3 of adulthood, levels of indicated proteins were assessed with immunoblotting. Immunoblot against Pas-7 served as loading control. (F) N2 worms were grown on empty vector control (ev) or β -NAC RNAi. On day 3 of adulthood, mRNA levels of indicated genes were assessed by means of quantitative reverse transcriptase-PCR (RT-PCR). Data are represented as mean \pm SD. A Student's *t* test was used to assess significance: **P* < 0.05, ***P* < 0.01; ns, not significant. *xbp-1sp* = *xbp-1* spliced. (G) *hsp-4p::GFP* ER stress reporter worms were grown on empty vector control (ev), β -NAC RNAi, β -NAC + SR β RNAi, or SR β RNAi, and GFP fluorescence was assessed on day 2 of adulthood (fig. S2A). BF, bright-field. Scale bar, 0.5 mm. (H) N2 worms were grown on empty vector control (ev) or indicated RNAi. On day 2 of adulthood, Hsp-4 levels were analyzed with immunoblotting. Actin served as loading control.

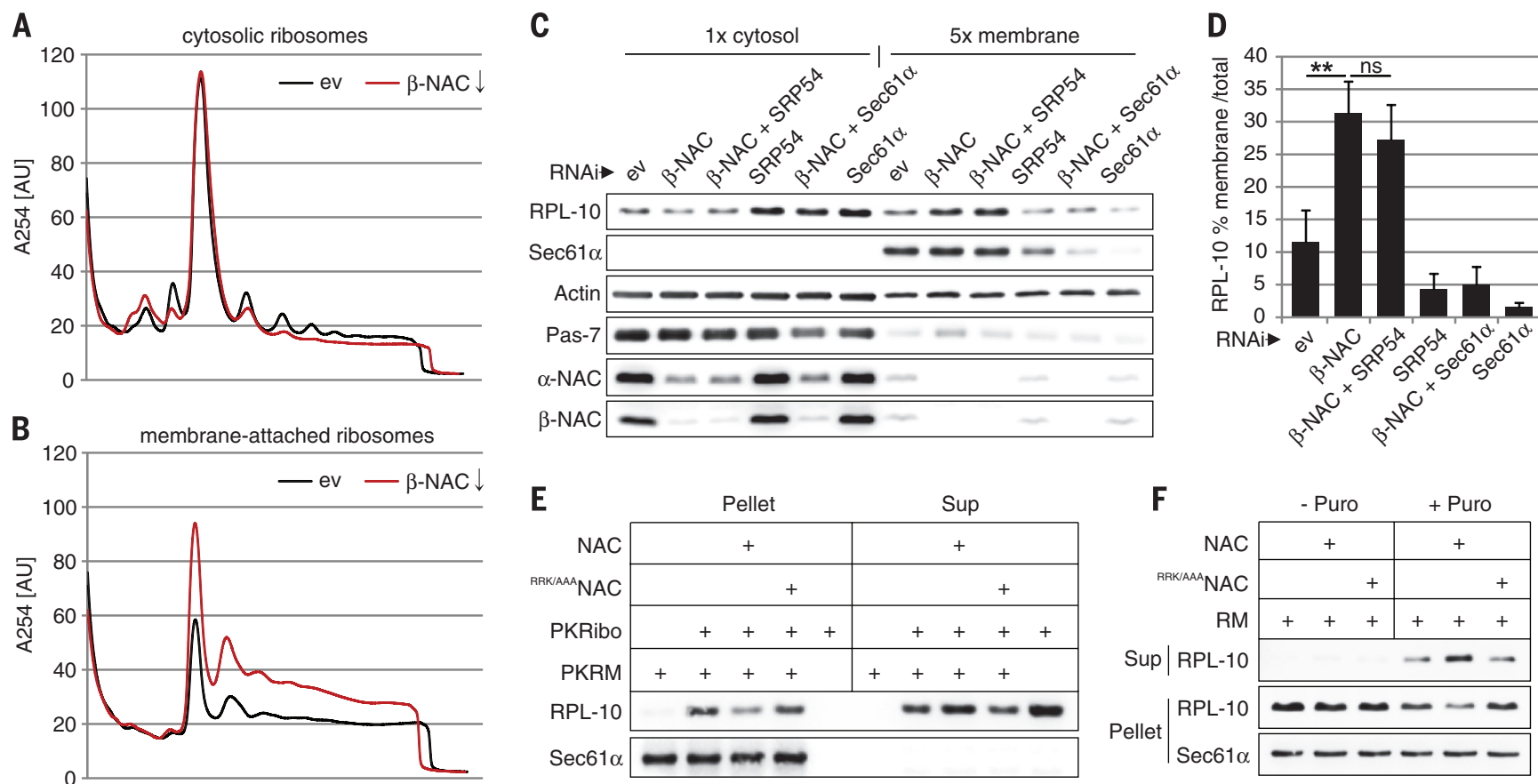


Fig. 2. NAC prevents SRP-independent ribosome-translocon binding. (A) Cytosolic polysome profiles of day-3 adult N2 worms grown on empty vector control (ev, black) or β-NAC RNAi (red). (B) Polysome profiles of membrane-attached ribosomes from animals as in (A). (C) N2 worms were grown on empty vector control (ev) or indicated RNAi. On day 3 of adulthood, indicated protein levels in cytosolic and membrane fractions were assessed with immunoblotting. Membrane fraction was loaded in fivefold excess over cytosolic fraction (5× membrane). Actin and Pas-7 served as loading controls (fig. S3, A and B). (D) Diagram shows percentage of membrane-bound ribosomes by means of RPL-10 levels in the cytosolic and membrane fractions shown as in

(C). Data are represented as mean ± SD. A Student's *t* test was used to assess significance: ***P* < 0.01; ns, not significant. (E) Puromycin and high salt-stripped ribosomes (PKRibo) and microsomes (PKRM) were incubated in the presence and absence of recombinant NAC or the ribosome-binding mutant ^{RRK/AAA}NAC (fig. S4). Microsomes were pelleted, and bound ribosomes were analyzed by means of RPL-10 levels. Sup, supernatant. (F) Native rough microsomes (RM) were treated with puromycin (Puro) in the presence and absence of recombinant NAC or ^{RRK/AAA}NAC. Microsomes were pelleted. Bound and released ribosomes were analyzed in the pellet and supernatant (Sup), respectively, with immunoblot analysis of RPL-10.

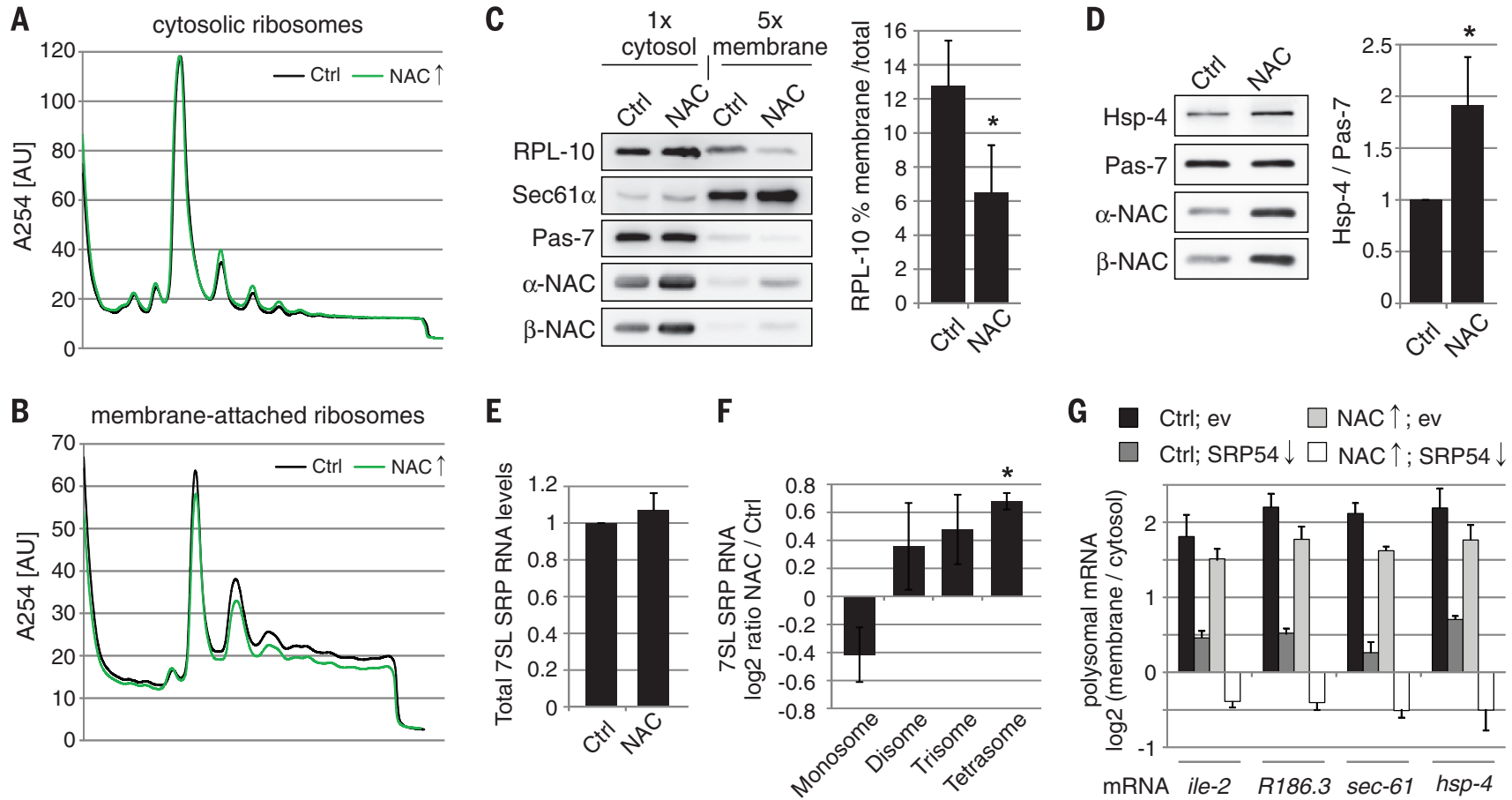


Fig. 3. NAC overexpression interferes with SRP-dependent ER targeting.

(A) Cytosolic polysome profiles of day-2 adult control (Ctrl, black) and NAC-overexpressing worms (green). (B) Polysome profiles of membrane-attached ribosomes from animals as in (A). (C) Control (Ctrl) and NAC-overexpressing worms were harvested on day 2 of adulthood, and indicated protein levels in cytosolic and membrane fractions were assessed with immunoblotting. Membrane fraction was loaded in fivefold excess over cytosolic fraction (5x membrane). Pas-7 served as loading control. (D) Total extracts of animals as in (C) were prepared and indicated proteins were analyzed with immunoblotting. Pas-7 served as loading control. (E) Control (Ctrl) and NAC-overexpressing worms were harvested on day 2 of adulthood, and total 7SL

SRP RNA levels were assessed by means of quantitative RT-PCR. Data are represented as mean ± SD. (F) Monosome, disome, trisome, and tetrasome fractions of ribosome sedimentation analysis shown as in (A) were collected, and 7SL SRP RNA levels were assessed by means of quantitative RT-PCR. Data are represented as mean ± SD. A Student's *t* test was used to assess significance: **P* < 0.05. (G) Control (Ctrl) and NAC-overexpressing worms were grown on empty vector control (ev) or SRP54 RNAi. On day 3 of adulthood, the distribution of indicated ribosome-associated mRNAs between cytosol and ER membrane was assessed by means of quantitative RT-PCR. Depicted is the log₂-transformed membrane-to-cytosol ratio for indicated mRNAs. Data are represented as mean ± SD.

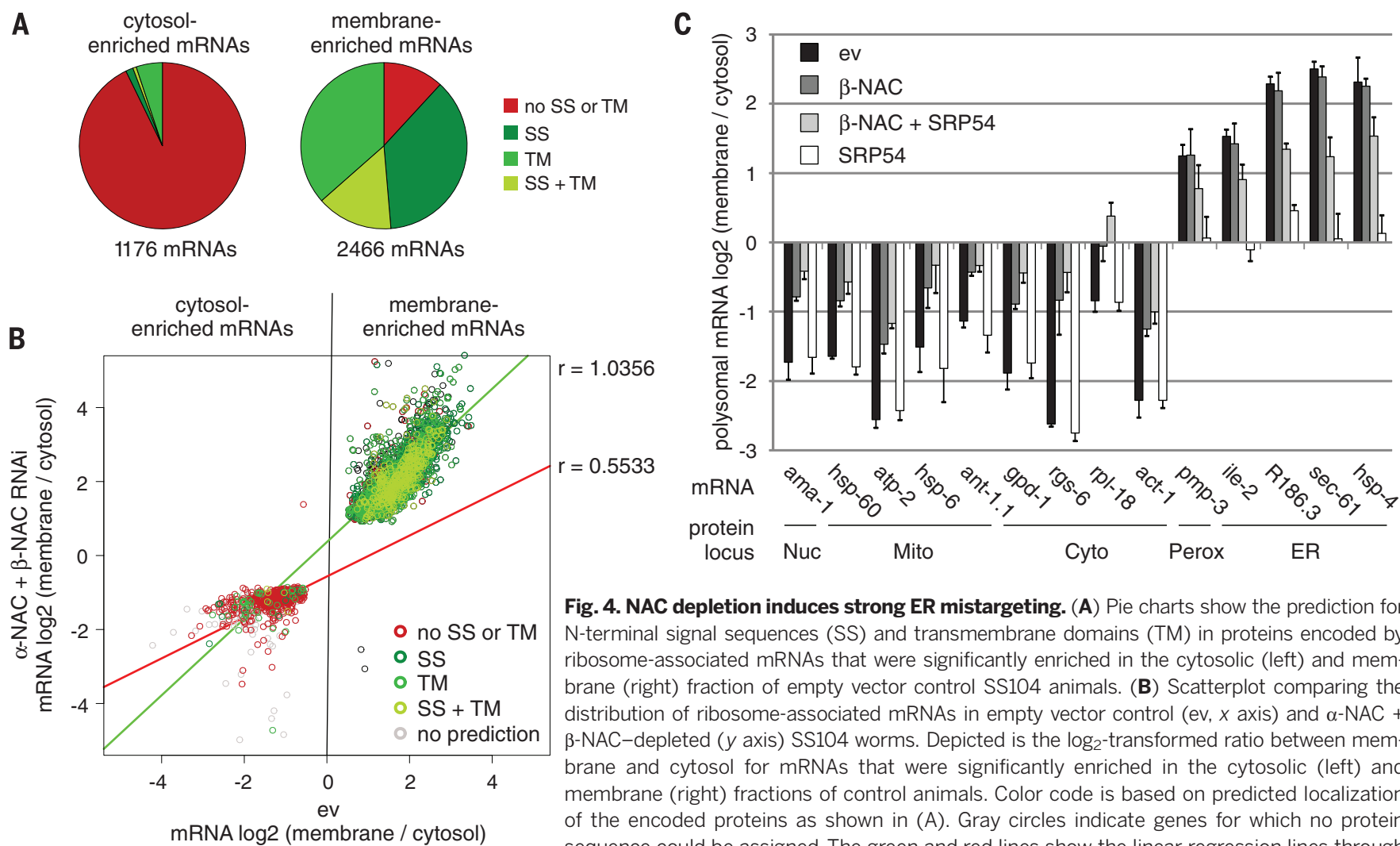


Fig. 4. NAC depletion induces strong ER mistargeting. (A) Pie charts show the prediction for N-terminal signal sequences (SS) and transmembrane domains (TM) in proteins encoded by ribosome-associated mRNAs that were significantly enriched in the cytosolic (left) and membrane (right) fraction of empty vector control SS104 animals. (B) Scatterplot comparing the distribution of ribosome-associated mRNAs in empty vector control (ev, x axis) and α -NAC + β -NAC-depleted (y axis) SS104 worms. Depicted is the log₂-transformed ratio between membrane and cytosol for mRNAs that were significantly enriched in the cytosolic (left) and membrane (right) fractions of control animals. Color code is based on predicted localization of the encoded proteins as shown in (A). Gray circles indicate genes for which no protein sequence could be assigned. The green and red lines show the linear regression lines through membrane- and cytosol-enriched mRNAs, respectively. (C) N2 worms were grown on empty vector control (ev) or indicated RNAi. On day 3 of adulthood, the distribution of indicated ribosome-associated mRNAs between cytosol and ER membrane was assessed by means of quantitative RT-PCR. Depicted is the log₂-transformed membrane-to-cytosol ratio for select mRNAs coding for proteins with destination in the nucleus (Nuc), mitochondria (Mito), cytosol (Cyto), peroxisomes (Perox), and ER. Data are represented as mean \pm SD.

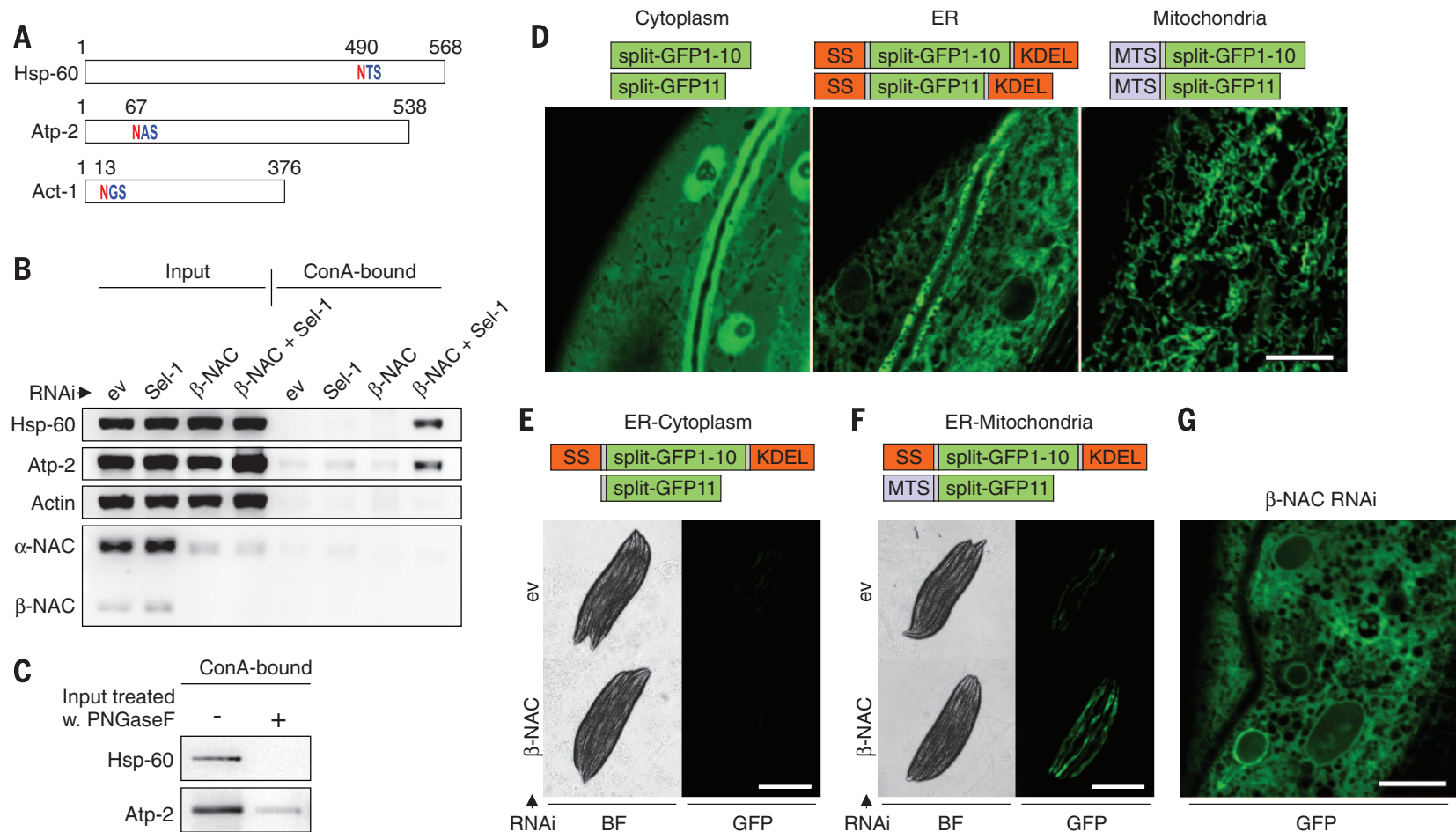


Fig. 5. Mitochondrial proteins are mislocalized to the ER and degraded by ERAD upon NAC depletion. (A) Schematic illustration showing predicted *N*-glycosylation sites in the mitochondrial proteins Hsp-60 and Atp-2 and the cytosolic protein Act-1. Predictions were performed with NetNGlyc 1.0. (B) N2 worms were grown on empty vector control (ev) or indicated RNAi. On day 3 of adulthood, glycosylated proteins were isolated by using the lectin Concanavalin A (ConA), and the levels of indicated proteins in the total extract (Input) and the lectin-bound fraction were analyzed with immunoblotting. (C) Total extracts (Input) of N2 worms grown on β -NAC + Sel-1 RNAi were treated or not with the *N*-glycosidase PNGaseF followed by Concanavalin A (ConA) affinity purification. The levels of ConA-bound Hsp-60 and Atp-2 were then assessed with immunoblotting. (D) Fluorescent micrographs of intestinal cells in worms expressing complementing split-GFP fragments in the cytoplasm (left), in the ER (middle) and in mitochondria (right). Scale bar, 10 μ m. SS, ER-specific signal sequence; KDEL, ER retention motif; MTS, mitochondrial targeting sequence. (E) Transgenic worms expressing split-GFP1-10 in the ER and split-GFP11 in the cytoplasm were grown on empty vector control (ev) or β -NAC RNAi, and GFP fluorescence was assessed on day 2 of adulthood. BF, bright-field. Scale bar, 0.5 mm. (F) Transgenic worms expressing split-GFP1-10 in the ER and split-GFP11 in mitochondria were grown on empty vector control (ev) or β -NAC RNAi, and GFP fluorescence was assessed on day 2 of adulthood. BF, bright-field. Scale bar, 0.5 mm. (G) Fluorescent micrograph of intestinal cells in β -NAC-depleted worms as shown in (F). Scale bar, 10 μ m.

tinal cells in worms expressing complementing split-GFP fragments in the cytoplasm (left), in the ER (middle) and in mitochondria (right). Scale bar, 10 μ m. SS, ER-specific signal sequence; KDEL, ER retention motif; MTS, mitochondrial targeting sequence. (E) Transgenic worms expressing split-GFP1-10 in the ER and split-GFP11 in the cytoplasm were grown on empty vector control (ev) or β -NAC RNAi, and GFP fluorescence was assessed on day 2 of adulthood. BF, bright-field. Scale bar, 0.5 mm. (F) Transgenic worms expressing split-GFP1-10 in the ER and split-GFP11 in mitochondria were grown on empty vector control (ev) or β -NAC RNAi, and GFP fluorescence was assessed on day 2 of adulthood. BF, bright-field. Scale bar, 0.5 mm. (G) Fluorescent micrograph of intestinal cells in β -NAC-depleted worms as shown in (F). Scale bar, 10 μ m.

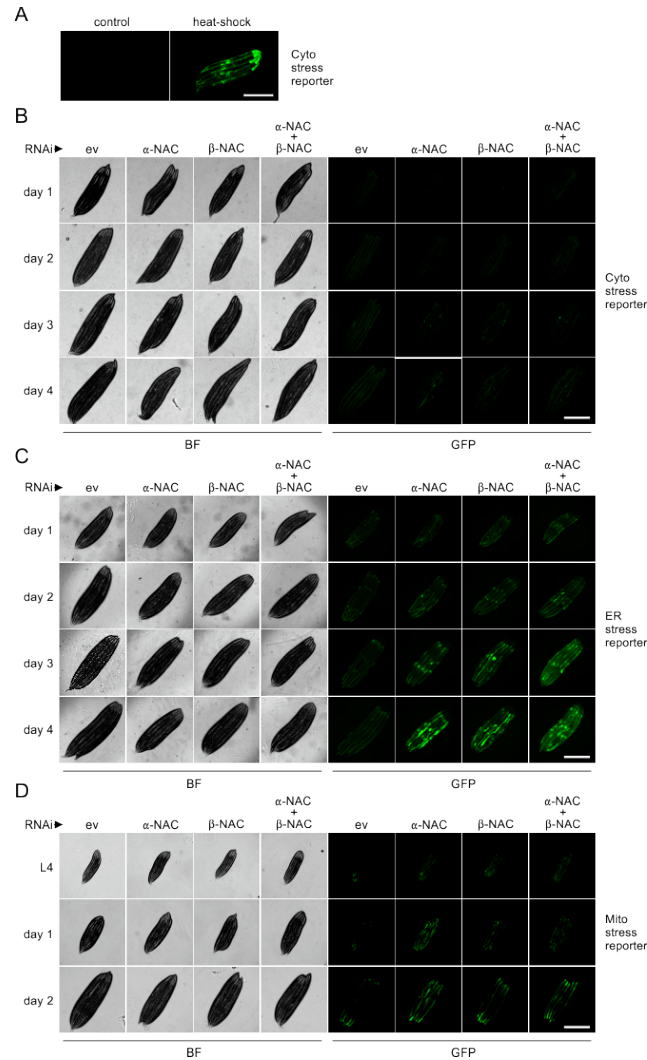


Fig. S1 NAC depletion induces ER and mitochondrial stress

(A) *hsp-16.2p::GFP* cytosolic stress reporter worms were heat-shocked for 90 min at 35°C and GFP fluorescence was assessed after 6 hours of recovery at 20°C. (B) *hsp-16.2p::GFP* cytosolic stress reporter worms were grown on empty vector control (ev) or indicated RNAi. GFP fluorescence was assessed from day 1 to day 4 of adulthood. (C) *hsp-4p::GFP* ER stress reporter worms were grown on empty vector control (ev) or indicated RNAi and GFP fluorescence was assessed from day 1 to day 4 of adulthood. (D) *hsp-6p::GFP* mitochondrial stress reporter worms were grown on empty vector control (ev) or indicated RNAi and GFP fluorescence was assessed from the last larval stage (L4) to day 2 of adulthood. BF = Bright-field. Scale bar = 0.5 mm.

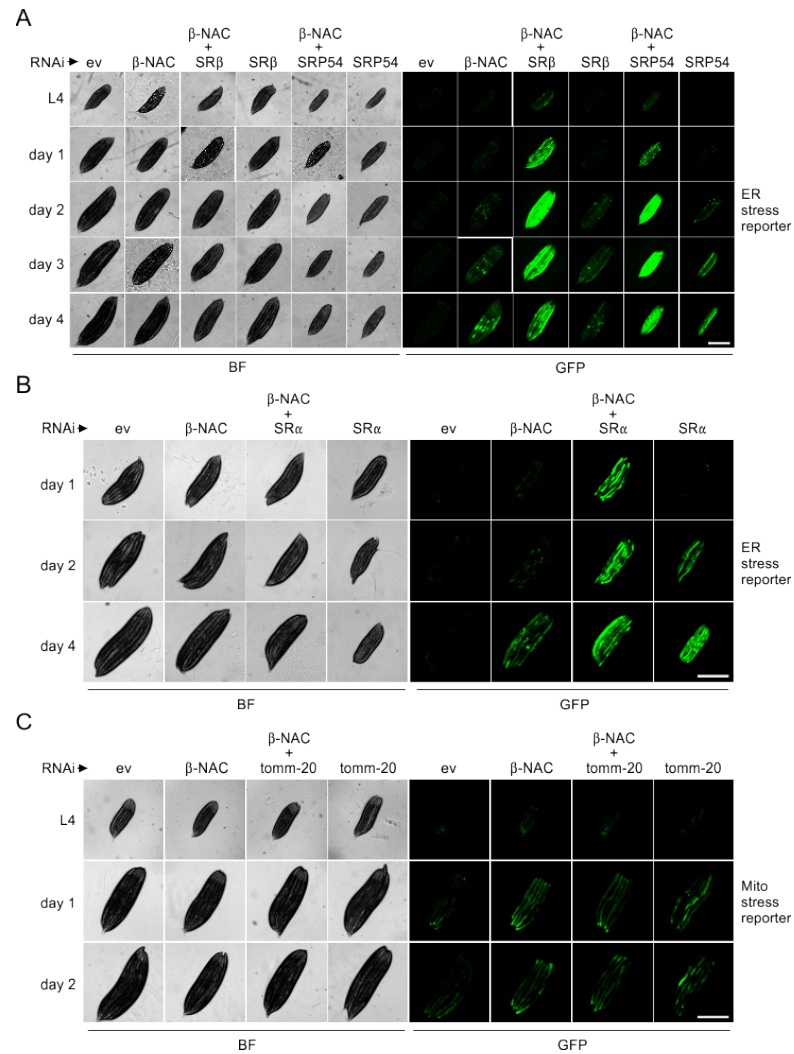


Fig. S2 Impairment of the SRP pathway potentiates the ER stress response in NAC depleted animals.

(A) *hsp-4p::GFP* ER stress reporter worms were grown on empty vector control (ev) or indicated RNAi and GFP fluorescence was assessed from the last larval stage (L4) to day 4 of adulthood. (B) *hsp-4p::GFP* ER stress reporter worms were grown on empty vector control (ev), β -NAC, β -NAC + SR α , or SR α RNAi and GFP fluorescence was assessed from day 1 to day 4 of adulthood. (C) *hsp-6p::GFP* mitochondrial stress reporter worms were grown on empty vector control (ev) or indicated RNAi and GFP fluorescence was assessed from the last larval stage (L4) to day 2 of adulthood. BF = Bright-field. Scale bar = 0.5 mm.

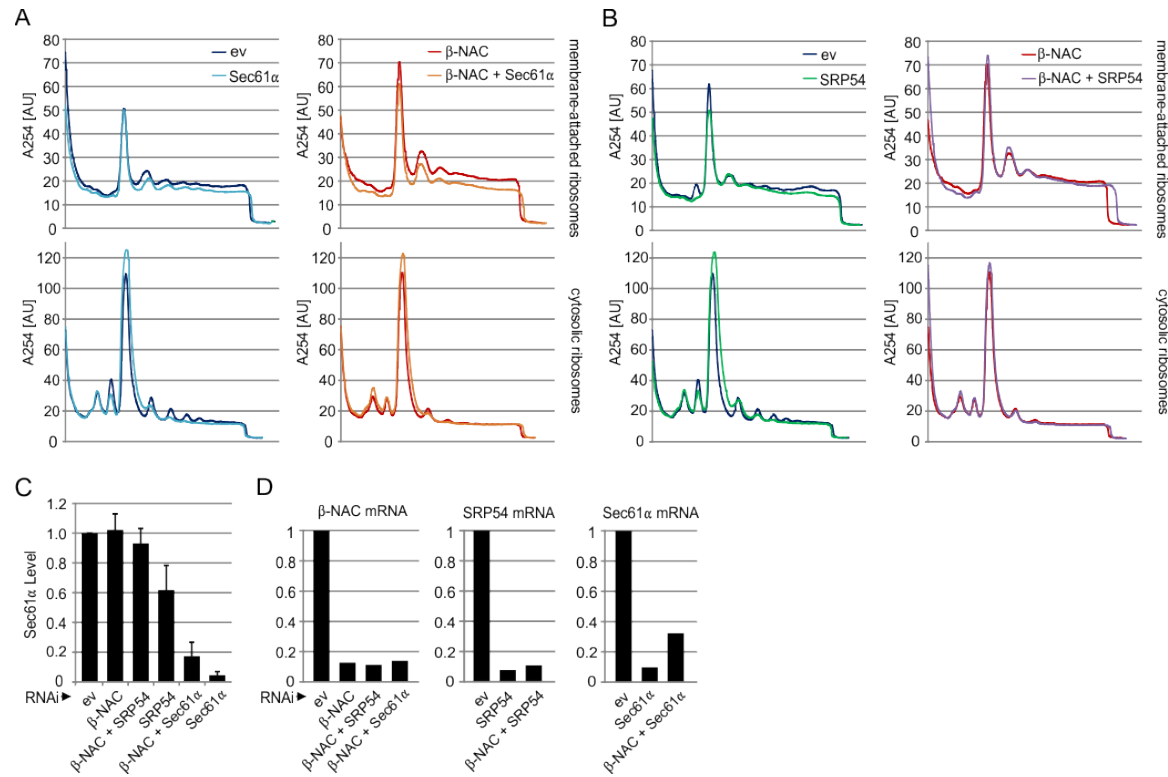


Fig. S3 NAC depletion leads to increased, SRP-independent binding of ribosomes to ER translocons

(A) N2 worms were grown on empty vector control (ev, dark blue), Sec61α RNAi (light blue), β-NAC RNAi (red) or β-NAC + Sec61α RNAi (orange). On day 3 of adulthood polysome profiles of membrane-attached (upper panels) and cytosolic (lower panels) ribosomes were assessed. (B) N2 worms were grown on empty vector control (ev, dark blue), SRP54 RNAi (green), β-NAC RNAi (red) or β-NAC + SRP54 RNAi (violet). On day 3 of adulthood polysome profiles of membrane-attached (upper panels) and cytosolic (lower panels) ribosomes were assessed. (C) Quantification of Sec61α levels assessed by immunoblotting shown as in Figure 2C. Data are represented as mean ± SD. (D) Knockdown efficiencies of RNAi experiment shown in Figure 2C measured by means of quantitative RT-PCR.

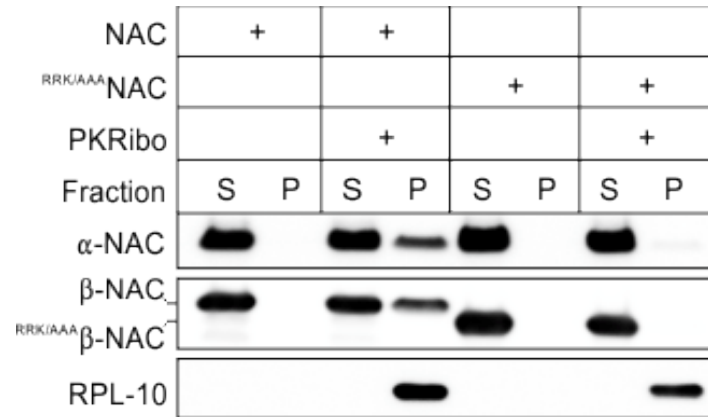


Fig. S4 Ribosome sedimentation assay testing the binding of WT-NAC and ^{RRK/AAA}-NAC to ribosomes

Puromycin and high salt-stripped ribosomes (PKRibo, 0.5 μ M) were incubated with WT-NAC or mutant ^{RRK/AAA}NAC (8 μ M), in which the evolutionary conserved RRK motif in β -NAC, that is critical for ribosome binding (34), was mutated to AAA. Ribosomes were pelleted through a sucrose cushion by ultracentrifugation and bound and unbound NAC was assessed in the pellet (P) and supernatant (S), respectively, by immunoblot analysis. Note that ^{RRK/AAA} β -NAC migrates faster than WT- β -NAC in SDS-PAGE due to charge variation.

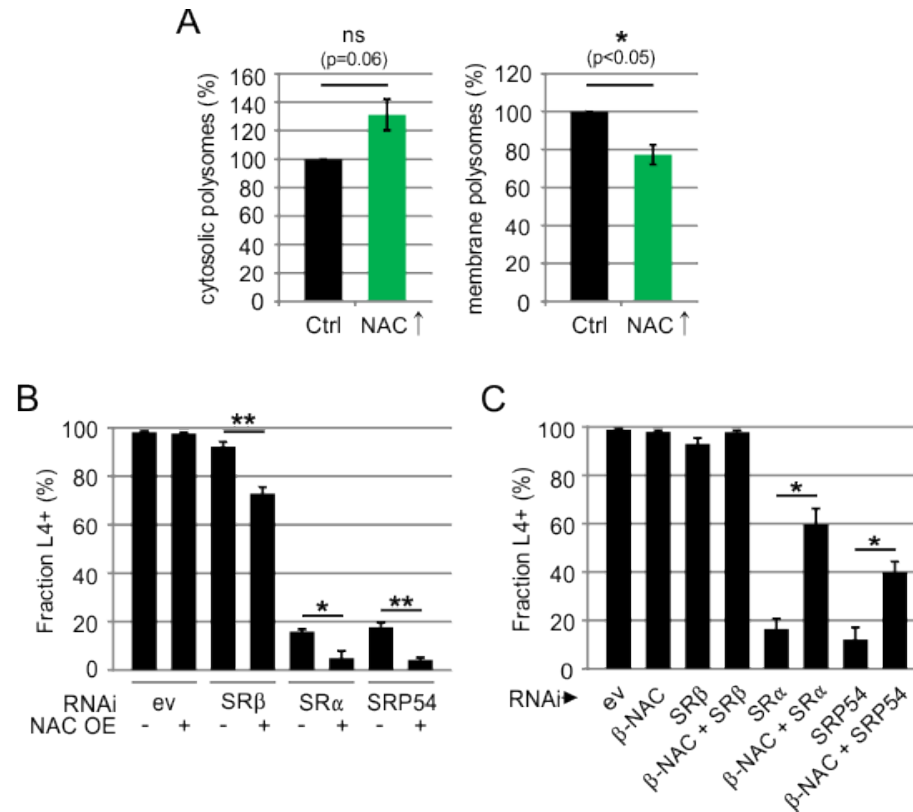


Fig. S5 NAC overexpression interferes with SRP-dependent targeting

(A) Polysome quantifications of cytosolic and membrane ribosome profiles of control (Ctrl) and NAC-overexpressing worms (NAC↑) shown as in Fig. 3A, B. Polysomal peaks were quantified using Image J. Data are represented as mean ± SD. A Student's t test was used to assess significance: *p < 0.05; n = 3. ns = not significant. (B) Control (-) and NAC overexpressing L1 larvae (+) were grown on empty vector control (ev) or indicated RNAi. After 4 days, the fraction of adult animals (L4+) was assessed. Data are represented as mean ± SD. A Student's t test was used to assess significance: *p < 0.05, **p < 0.01. OE = overexpression. (H) N2 worms (L1 larvae) were grown on empty vector control (ev) or indicated RNAi. After 4 days, the fraction of adult animals (L4+) was assessed. Data are represented as mean ± SD. A Student's t test was used to assess significance: *p < 0.05.

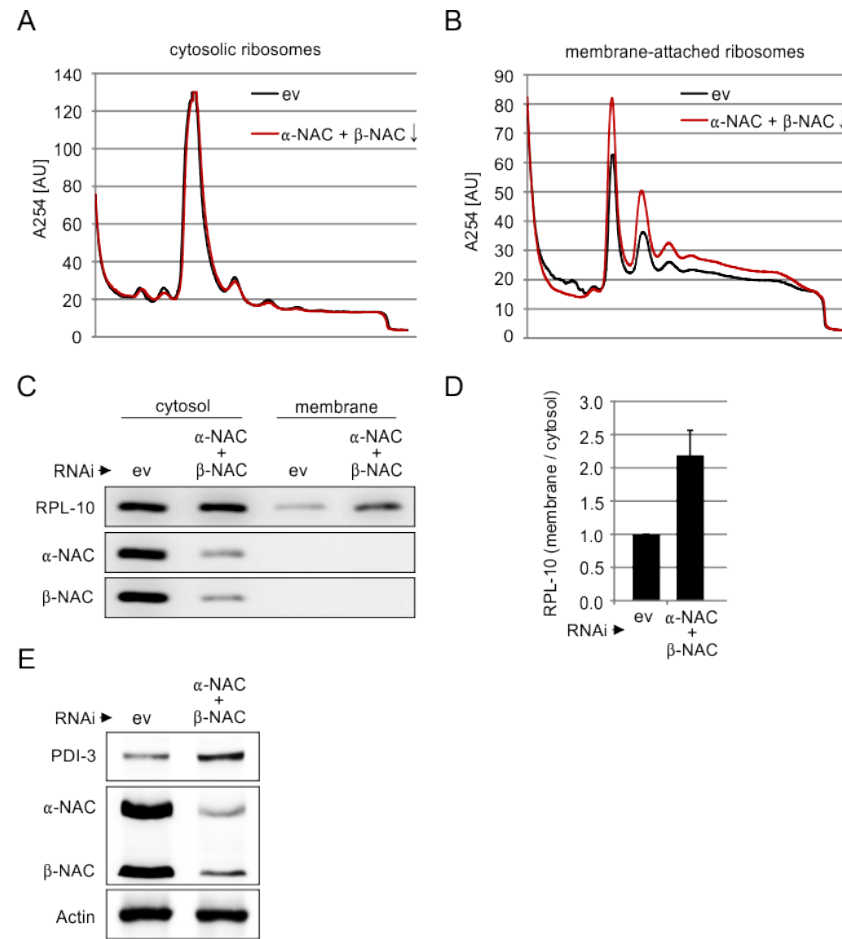


Fig. S6 NAC RNAi phenotype in temperature-sensitive sterile mutants

(A) Temperature sensitive sterile mutants (SS104) were grown at the nonpermissive temperature on empty vector control (ev, black) or α -NAC + β -NAC RNAi (red). On day 3 of adulthood polysome profiles of cytosolic ribosomes were assessed. (B) Polysome profile of membrane-attached ribosomes from animals as in (A). (C) Ribosomal fractions of sedimentation analyses shown in (A) and (B) were collected and subjected to immunoblot analysis of indicated proteins. (D) Diagram shows the membrane-to-cytosol ratio of ribosomes by means of RPL-10 levels in the cytosolic and membrane fractions shown as in (C). Ratio of empty vector control (ev) worms was set to one. Data are represented as mean \pm SD. (E) Total extracts of animals as in (A) were prepared and indicated proteins were analyzed by immunoblotting. Actin served as loading control.

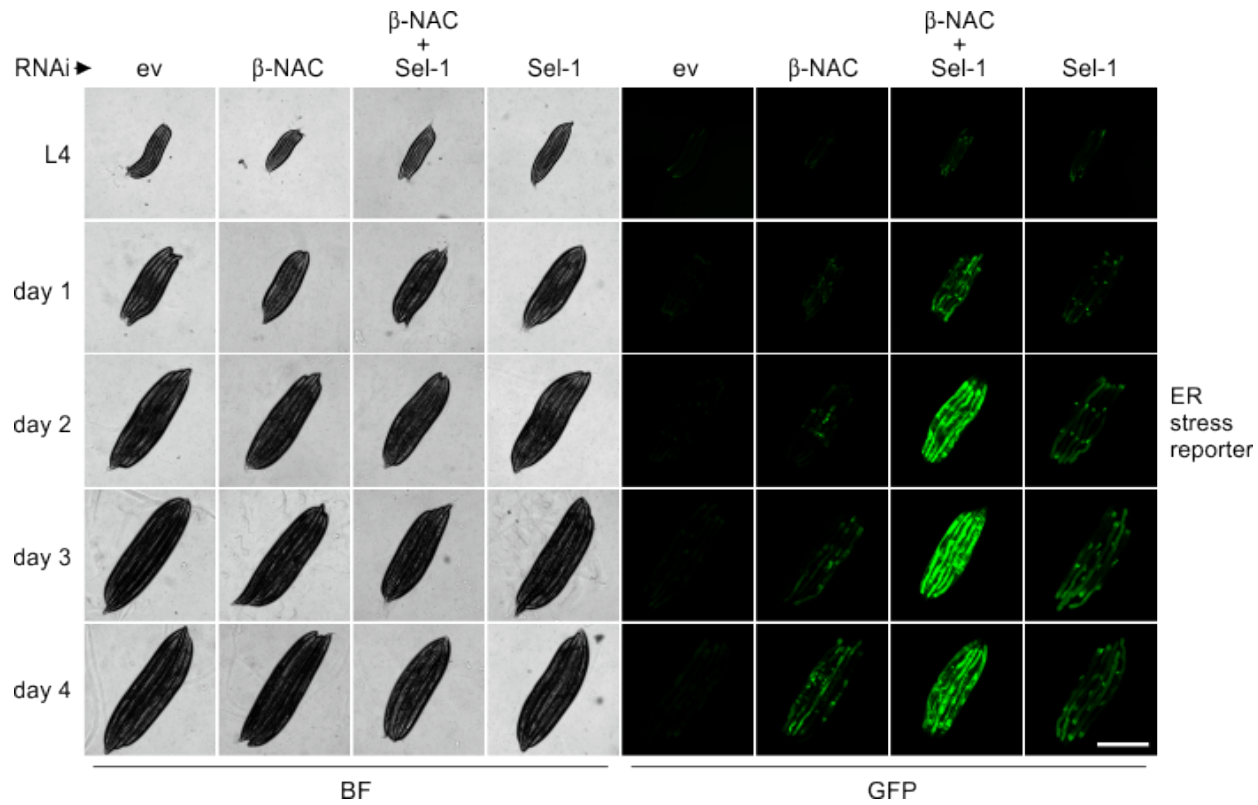


Fig. S7 Impairment of the ERAD pathway increases the ER stress response in NAC depleted animals

hsp-4p::GFP ER stress reporter worms were grown on empty vector control (ev) or indicated RNAi and GFP fluorescence was assessed from the last larval stage (L4) to day 4 adulthood. BF = Bright-field. Scale bar = 0.5 mm.